



# Geoblocks Delineation and Recognition of Earthquake Prone Areas in the Tuan Giao Area (Northwest Vietnam)

Nguyen Huu Tuyen<sup>1</sup>, Pham Nam Hung<sup>2</sup>, Cao Dinh Trong<sup>2</sup>, Nguyen Trung Thanh<sup>3</sup>,  
Phung Van Phach<sup>3</sup>, Renat Shakirov<sup>4</sup>

<sup>1</sup>Department of Tectonophysics, Institute of Geophysics, VAST, A8, 18 Hoang Quoc Viet, Nghia Do, Cau Giay Hanoi, Vietnam

<sup>2</sup>Departments of Geodynamic, Institute of Geophysics, VAST, A8, 18 Hoang Quoc Viet, Nghia Do, Cau Giay Hanoi, Vietnam

<sup>3</sup>Institute of Marine Geology and Geophysics, VAST, A27, 18 Hoang Quoc Viet, Nghia Do, Cau Giay Hanoi, Vietnam

<sup>4</sup>Gasgeochemistry Laboratory, V. I. Il'ichev Pacific Oceanological Institute, Far Eastern Branch, Russian Academy of Sciences, Vladivostok, Russian Federation

## Email address:

tuyennh@igp-vast.vn (N. H. Tuyen)

## To cite this article:

Nguyen Huu Tuyen, Pham Nam Hung, Cao Dinh Trong, Nguyen Trung Thanh, Phung Van Phach, Renat Shakirov. Geoblocks Delineation and Recognition of Earthquake Prone Areas in the Tuan Giao Area (Northwest Vietnam). *American Journal of Environmental and Resource Economics*. Vol. 2, No. 3, 2017, pp. 132-150. doi: 10.11648/j.ajere.20170203.16

**Received:** May 24, 2017; **Accepted:** June 3, 2017; **Published:** July 24, 2017

---

**Abstract:** The goal of the paper is to delineate the hierarchical block- structure in the Tuan Giao area (Northwest Vietnam) and, on that base, to identify earthquake prone areas for M5+. Four large geoblocks of the second rank have been delineated on the basis of the joint analysis of geological, geophysical, geomorphic, and remote sensing data. The second rank geoblocks have been divided into smaller sub-blocks of the third rank. The recent geodynamics of the geoblocks have been characterized using geomorphic, seismological, gravity, and GPS data. The system of the delineated geoblocks is viewed as the Geodynamic Blocks model (GB). Earthquake prone areas for M5+ have been identified with the pattern recognition algorithm CORA-3. The objects of the recognition were defined as the circular areas where boundaries of the geoblocks intersect each other. The results of the recognition confirms high seismic potential of the study region and provides information on potential earthquake sources for seismic hazard assessment: a number of boundary intersections have been identified as prone to M5+ in the areas where events of such size are not recorded up to date.

**Keywords:** Geoblocks, Pattern Recognition, Earthquakes, Boundary Intersections, Tuan Giao

---

## 1. Introduction

The Tuan Giao area, located in Northwest Vietnam (figure 1), belongs to the northeast edge of the protruded Indochina block that borders the South China block along the deep Red River fault zone. The recent geodynamics of the study area is conditioned by the collision of the Indo - Australian plate into the Eurasian one, in northwest, and by the subduction of the Pacific plate beneath the Eurasian one, in the eastern edge. During the Cenozoic the intensity of the plate interaction was varied in different regions [Tapponnier, 1995; Trieu, 2002, 2005; Tuyen H. N., 2012;]. The complicated tectonic regime caused the large horizontal displacements of the Red River fault zone evidenced in the sinistral strike slip with the offset of 500 – 700 km (pre Miocene) and in the dextral strike slip with the amplitude of 5,5 km (from the

Pliocene to present) [Tapponnier, 1995]. The active tectonic processes governs the moderate to strong seismicity in the region including the 1935 Dien Bien earthquake, Ms = 6.8 and the 1983 Tuan Giao earthquake, Ms = 6.7 [Trieu and Nguyen 2006, 2008; Thuy N. N 2005; Tuyen N. H 2012; Tuyen N. H et al., 2012].

According to the plate tectonics, the Earth' lithosphere consists of a number of the major plates and the sub- plates (*micro-plates*) divided by boundaries of different type: subduction zones, ocean - spreading ridges, transform faults [Le Pichon et al., 1973]. Using the idea on the block-structure of the crust originating from the plate tectonics it is possible to divide the region into a system of the geoblocks and sub-blocks at the regional scale. The block-structure of the Tuan Giao area has been intensively studied during last years with a goal to delineate geoblocks and define their

distinguishing tectonic features [Trieu and Nguyen 2006, 2008; Tuyen N. H and Chu V. N., 2010; Tuyen N. H et al., 2012a]. The studies of the Tuan Giao area permitted to formulate a new concept on the Geodynamic geoblocks [Tuyen N. H et al., 2012a].

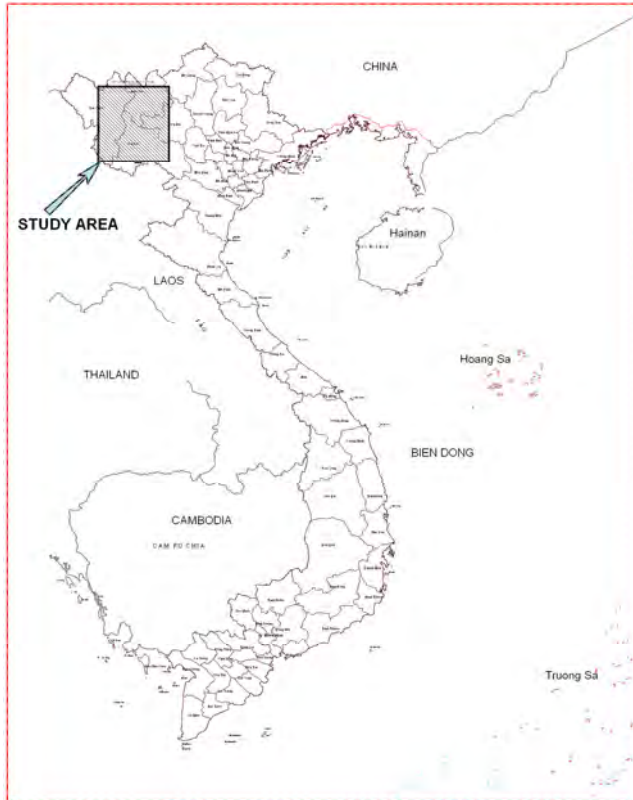


Figure 1. Study area of Tuan Giao.

Since earthquakes are generated by block interaction along the systems of faults, the study of the block-structure is the essential precondition for seismic hazard analysis. One of the most advanced methodologies for identifying the earthquake prone areas [Gelfand et al., 1972; Gorshkov et al., 2003] is also based on the idea on the block-structure of the crust. In the framework of this methodology the block-structure is delineated with the morphostructural zoning method (MZ) enabling to delineate hierarchical system of blocks divided by morphostructural lineaments, the intersections (nodes) of which control the spatial distribution of strong earthquakes [Alexeevskaya et al., 1977; Rantsman, 1979; Gorshkov et al., 2003]. The long-term worldwide application of the methodology [Gelfand et al., 1972; Gorshkov et al., 2000, 2003, 2004, 2009, 2010; Gvishiani et al., 1987, 1988] demonstrated its sufficiently high affectivity for identification of earthquake prone areas [Soloviev et al., 2104]. Most recently, this methodology has been applied for identifying seismogenic nodes capable of earthquakes M5+ in North Vientnam [Tuyen N. H et al., 2012b].

The goal of this work is to delineate the hierarchical system of the geodynamic geoblocks (GB) in the Tuan Giao and adjacent areas with analyzing the integrated data set including geomorphic, geological, gravity, seismological,

and remote sensing data.. The created GB model reflects the recent tectonic activity, geodynamic behavior, accumulated stress of the geoblocks as well as the interaction between them. Because of this, the GB model provides the irreplaceable base for studying different geohazard phenomenon including earthquakes, subsidence, landslides, liquefaction etc. In this work, the GB model is employed for identifying earthquake prone areas capable of events with M5+ using the pattern recognition algorithm CORA-3 [Gelfand et al., 1972; Gorshkov et al., 2003].

The study area is limited of 21°00 – 22°30 N in latitude and 103°00 – 104°30 E in longitude (figure 1).

## 2. Principles of Geoblocks Classification

### 2.1. Main Principles of Geoblocks Delineation

According to the plate tectonics the Earth's lithosphere, on the global scale, consists of several major plates and micro-plates. On a regional scale, these large-scale plates are continuously can be divided into lower level structures such as geoblocks which differ markedly from each other by different characteristics. In turn, geoblocks can be divided into smaller sub-blocks, separated by boundaries which intersect each other. The boundaries between blocks are presented by faults along of which blocks move with respect to each other. Thus, "Geoblock" is the model postulating that the geodynamics of the lithosphere reveals in the relative movements of blocks and sub-blocks along their boundaries.

At the local scale, the structural geodynamics units by analogy with the plate tectonics are divided into block structures limited by the boundaries of the same rank. For example, the lithospheric plate is consistent with their boundaries presented by *subduction zones, ridges, transform faults*. The micro-plate is consistent with the boundaries presented by *metamorphic deformation range, spreading rift, collision zone*). The block - block classification is consistent with the fault/lineament boundaries. The sub-block classification is consistent with the fault boundaries of the smaller rank. The boundaries of the structure include faults and and their intersections,"nodes". Therefore, geoblocks differ from each other by different characteristics determined by the analysis different integrated data set. The delineated structural units (*geoblocks*) are characterized by the relative homogeneity of the geological environments, lithological parameters, geophysical fields, and the stress state. In addition, in terms of dynamics and kinematics each geodynamic structural unit differ from the adjacent geodynamics blocks in the rate and orientation of the relative movements.

*Geoblock* is an unit characterized by a relative uniformity of geological, lithological, and geophysical characteristics, which differ from the same characteristics in the adjacent structural units. The integrated analysis of the data set allows delineating the individual structural units and their boundaries separating them from the neighboring units. Applied to the Tuan Giao area the structural units can be

grouped in the hierarchical blocks system that includes the blocks of the first (I), second (II) and third (III) ranks.

*Boundaries of the Geoblocks*, Each block is separated from the others by the boundaries presented by the fault zones, fracture or shear zones, and as well as by zones of the high deformations. The block of a certain rank is bounded by the boundaries of the same rank. The boundaries are connected spatially with the blocks but they are also the individual structural units. The boundaries are the transition zones between blocks, along of which blocks interact and move with respect to each other. The boundary zones are most likely sites for the occurrences of the geohazard phenomenon such as earthquakes, landslides, subsidence etc. Therefore the delineation of the boundaries system is important for the geohazard reduction.

*Intersecting structures*, this type of structures (*nodes*) is formed at sites where boundaries of different strikes intersect or join each other. The studies of the intersecting lineaments and fault zones have shown the close relationship between earthquakes and nodes [Gorshkov et al., 2000, 2003, 2004, 2009, 2010; Gvishiani et al., 1987, 1988; Hudnut et al., 1989; Tuyen N. H et al., 2010, 2012b; Talwani, 1988]. Therefore, the study of the intersecting structures in the Tuan Giao region is of great importance for evaluating earthquakes hazard and developing the preparedness measures.

## 2.2. Data Used for Geoblocks Delineation

According to the above principles, we have used the available set of detailed data that included geological, geophysical, topographic, geomorphic indicators for the interpretation of geodynamic conditions in the study region. We used three main groups of data for the identification of structural elements composing the final map of geodynamic blocks by overlaying all types of data. The following three groups of data have been analyzed:

1. This group includes data reflecting the material composition and the physical characteristics of the media including, the geological evidences, the magnetic, gravity, and isostatic anomalies, and the Poisson ratio. The homogeneous geophysical characteristics reflect the physical state and geodynamic conditions within each domain [Cao et al., 2002, 2005; Dang T. H, 2003; Tuyen N. H., 2012]. The typical structure of the mantle geodynamics were identified through the morphological analysis of the deep structural boundaries, the crystalline basement discontinuous, and the Conrad and Moho discontinuous.

2. This group includes data for studying the evidences detectable on the Earth' surface that express indirectly of the geodynamic processes taking place at the depth. These evidences reflect both the dynamic state and the activity level of a region [Edward et al., 1996; Korzhuev, 1974; Thang N. G, etc 2007; 2009; Lu et al., 2010; Turcotte and Schubert, 2002]. A number the characteristics have been considered as the specific criteria for the interpretation and regionalization of the geodynamic processes. Such characteristics include the variety of the crust thickness, density of lineament intersections, vertical deformations during the Pliocene-

Quaternary. The present-day topography is an indicator and direct result of the geodynamic processes which had been taken place at the depth. The following morphological features of the surface-topography were taken into account: differentiation of the terrain elevations, the distribution of the top and root surface erosion, Sinuosity index ( $S_{mf}$ ), the correlation between the width and height of the valley bottom ( $V_f$ ), the law of distribution of Quaternary sediments, hydrographic network system, the changes of the fluvial fence [Turcotte and Schubert, 2002. Yeats, 1977].

3. In addition, the other characteristics such as mineral water springs, hot-spring exposure, geothermal field, earthquakes distribution (including paleoearthquakes), and volcanoes were also analyzed for delineating the geoblocks and their boundaries. Some other related evidences for classifying the regional structural units of have been determined during the field works [Tuyen N. H, 2012].

### a) The Expression of Geoblocks in the Geophysical Discontinuities.

The theoretical background for the system analysis of the morphological and gravity anomalies is based on a direct relationship between the physical properties and morphological structure of geological objects. The direct reflection of the morphological structure and the intensity of the gravity anomalies and magnetic fields has been proved in previous studies [Cao et al., 2008, 2005; Dang T. H 2003; Thuy N. N, 2005].

The dynamic processes in the deep crust are represented by the distinct physically based characteristics. Therefore, the interpretation of geophysical data such as the magnetic, gravity, electricity, geothermal observations is helpful for the comprehensive view on the geodynamics of the study area. In this study, we use a combination of data from all three groups for delineating the geodynamic structures. Specifically, the criteria for the delineation and characterization of geodynamic blocks include the gravity anomalies and (elevated levels of different height), gradient standardized form, Poisson coefficients expressing the correlation between the magnetic and gravity anomalies, the boundaries of the main layers of the crust (crystalline basement, the Conrad and Moho discontinuities), the isostatic equilibrium.

The study area belongs to the first rank structure of Northwest domain (I), which is separated from the first rank of Northeast domain (I) by the large Red River fault zone [Allen, 1984; Cao D. T., 2008, 2005; An L. D., 1994; Thuy N. N, 2005].

Figure 2a shows that the Poisson coefficients are significantly different in each geoblock delineated in the study region. The 2<sup>nd</sup> Hoang Lien Son geoblock oriented in the NW- SE direction is characterized with the coefficient values in range of 0.1 - 1.0. The 2<sup>nd</sup> closed Red River geoblock belonging to the first rank Northeast unit (I) exhibit the values in range of 1.2 - 3.8. The 2<sup>nd</sup> Son La – Song Da geoblock located in southeast is characterized with the value ranging from 0.6 to 2.0. The 2<sup>nd</sup> Muong Te geoblock is characterized with the values in range of 2.2 - 3.6.

The isolines of the Poisson coefficient values show the

NW-SE orientation in the 2<sup>nd</sup> Red River, Hoang Lien Son, Son La – Song Da geoblocks located in the northeast part of the region, while the orientation of the isolines is changed toward to the EW direction in the Muong Te geoblock located in southwest part of the region (figure 2a). Such sharply change of the orintation can be explained by the influence of the deep Lai Chau- Dien Bien fault zones. The spatial distribution of the isolines the Poisson coefficient allows also to delineate the third 3<sup>rd</sup> rank geoblocks (*internal structures*), namely, the 3<sup>rd</sup> Phan Si Pan and the 3<sup>rd</sup> Tu Le geoblocks (figure 2a).

Figure 2b shows the map of the depth of the crystalline basement. It is seen that in the 2<sup>nd</sup> Red River geoblock the isolines of the depth are oriented in the NW - SE direction and the depth varies from 0.1 - 1.0 km. Meanwhile, the 2<sup>nd</sup> Hoang Lien Son geoblock located closely to the 2<sup>nd</sup> Red River geoblock is characterized by the larger depth of the basement ranging from 0.2 to 1.7 km. The 2<sup>nd</sup> Hoang Lien

Son geoblock is divided into the Phan Si Pan and Tu Le blocks of lower rank characterized by the depth of the basement of 0.1 - 0.3 km. In the 2<sup>nd</sup> Song Da - Son La geoblock the depth of the basement ranges from 1.5 - 5.0 km and the isokines of the depth are oriented in the NW-SE direction. The 2<sup>nd</sup> Song Da - Son La geoblock can be divided into eight smaller units of the third rank including the Hat Lot, Muong La, Thuan Chau, Quynh Nhai, Nam Mua, Pusam Cap, and Sin Ho units. In the southeast we have outlined the 2<sup>nd</sup> Song Ma and Sop Cop geoblocks where the depth of the basemen varies from 0.3 to 1.1 km and isolines of the depth are oriented in the NW - SE direction. These geoblocks are clearly separated from the 2<sup>nd</sup> geoblocks located in the southwest where the depth abruptly increases 1.3 - 2.5 km. Further to the west the 2<sup>nd</sup> Muong Te geoblock is characterized by the depth of 0.3 - 1.7 km; the isolines of the depth are oriented in the geoblock in the N-S direction.

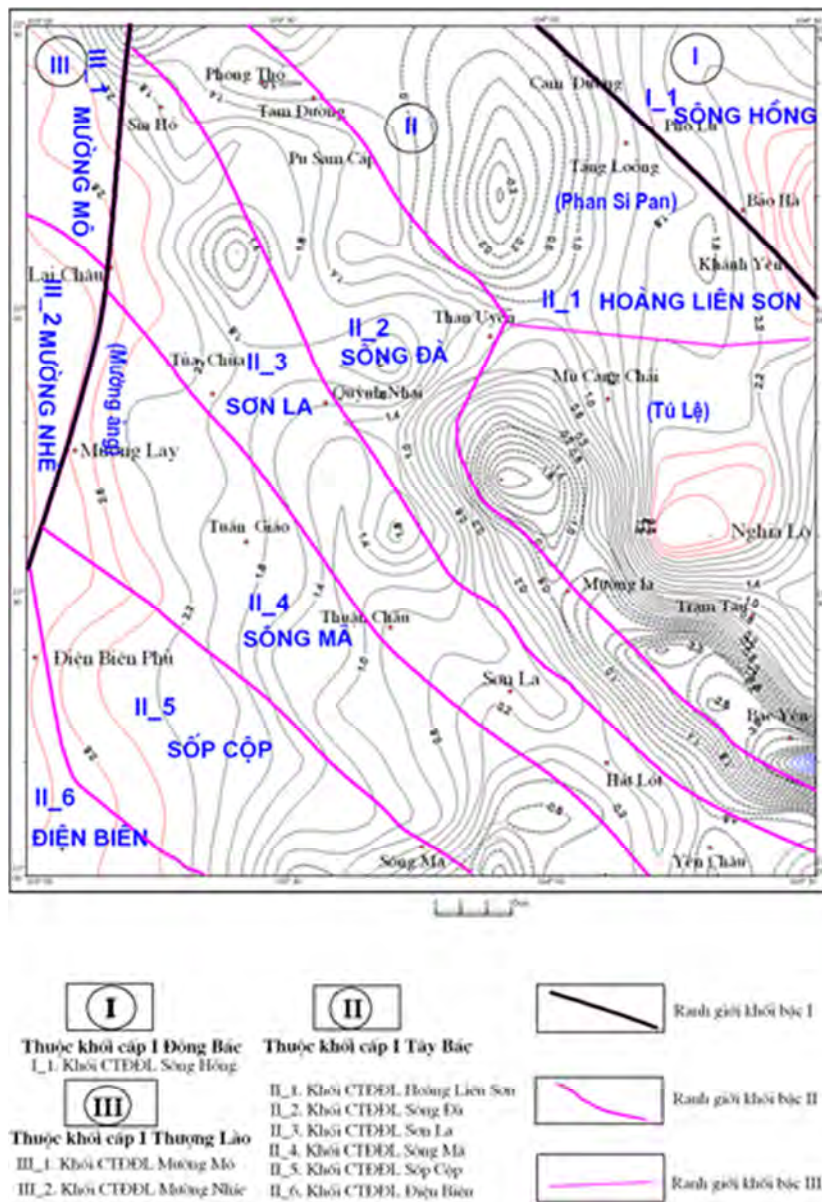


Figure 2a. The isolines of the Poisson coefficient in the Tuan Giao area.

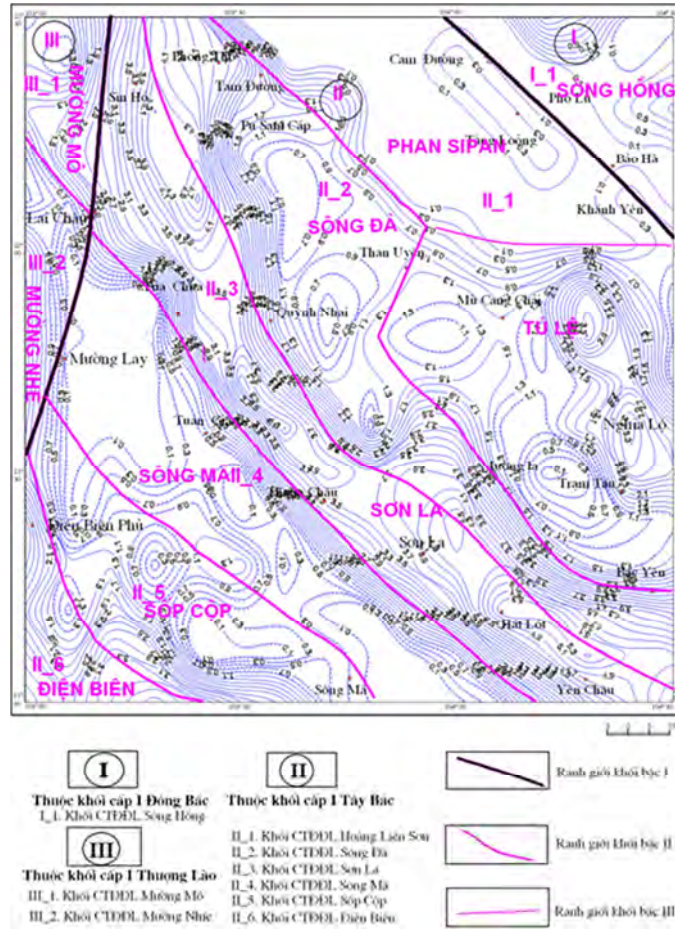


Figure 2b. Depth of the crystalline basement in Tuan Giao area.

Figures 3a and 3b show the Conrad and Moho discontinuities in the study region. We can see that the larger geoblocks are clearly expressed in these discontinuities, while the geoblocks of the lower rank are not clearly in these maps. The 2<sup>nd</sup> Red River geoblock is characterized by the Conrad depths of 15 - 17 km. The 2<sup>nd</sup> Hoang Lien Son geoblock is characterized by the Conrad depths in range of 8-18 km. On the detail level this 2<sup>nd</sup> geoblock is divided into low rank structures with different values of the Conrad depth. Specifically, we have outlined the Khanh Hung, Phan Si Pan, and Tu Le blocks characterized by the Conrad depth of 13 - 15 km, 16 - 18 km, and 8 - 13 km, correspondingly. Further to southwest, the 2<sup>nd</sup> Song Da – Son La and Song Ma geoblocks are identified by the Conrad depth that ranges from 9 to 15 km the Song Da – Son La geoblock and from 10 to 18 km in the Song Ma geoblock. In the other 2<sup>nd</sup> Sop Cop and Dien Bien geoblocks the Conrad depth varies from 9 to 12 km. The Moho depth is also different within each geoblocks. In the 2<sup>nd</sup> Hoang Lien Son geoblock varies from 22 to 36 km. In the 2<sup>nd</sup> Song Da - Son La geoblock the Moho depth varies from 26 - 32 km. In the 2<sup>nd</sup> Song Ma geoblock the depth is ranging from 28 to 32 km, while the 2<sup>nd</sup> Sop Cop and Dien Bien geoblocks are characterized by the similar depth in range of 27 - 31 km.

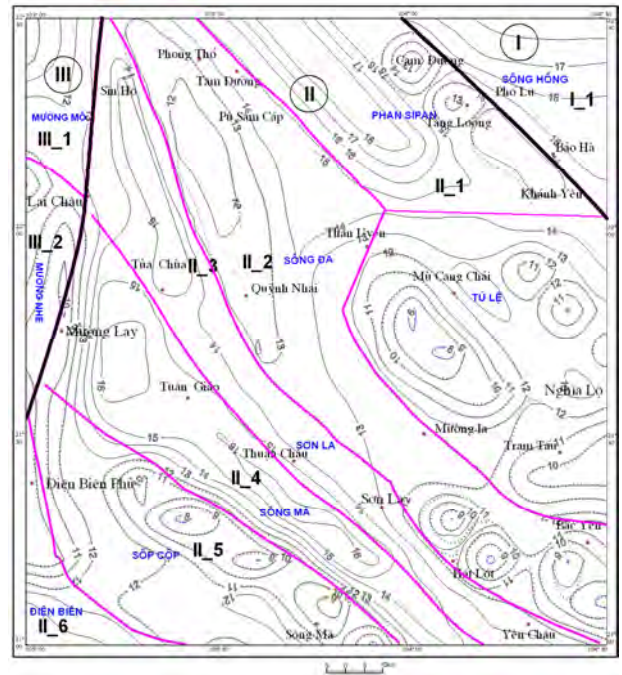


Figure 3a. The map of the Conrad discontinuity in Tuan Giao area.

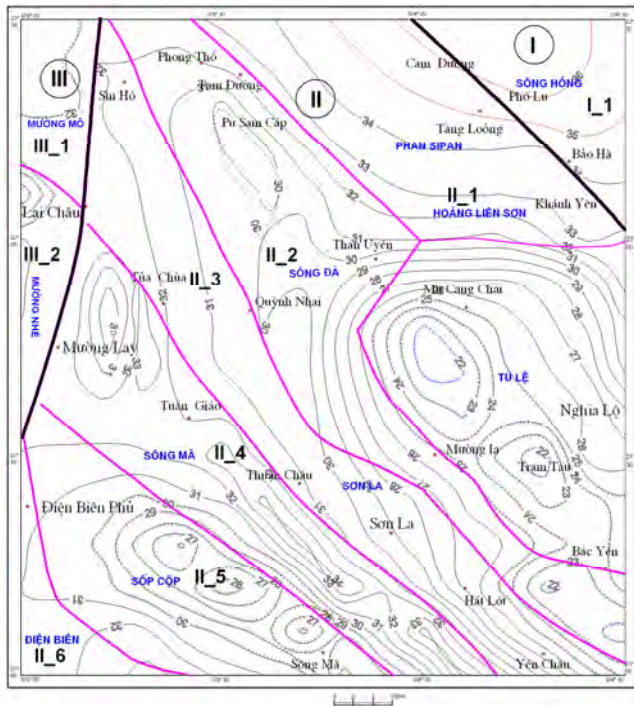


Figure 3b. The map of the Moho discontinuity in Tuan Giao area.

*b) Topographic and Geomorphologic Features of Geoblocks and Their Geodynamics Significance*

Through the analysis of geomorphological data we have identified the clearly expressed features of the geoblocks and their geodynamic characteristics. For this purpose, we have analyzed the topographic elevation, fracture zone trending, stamping down, deformation rate, and amplitude of the uplift. The present large landforms are, mainly, resulted from the tectonic evolution. Therefore the relief is dominated by the impact of the processes in the Earth's interiors. The active tectonics is conditioned by the thermal convection and gravity differentiated process beneath the earth crust. In other words, the internal processes seem to be the main factor responsible for the variations and changes in the present-day topography. Some evidences detectable on the Earth's surface indirectly reflect the geodynamic processes in the Earth's crust. The analysis of the landforms in combination with geological data has been used in this study.

The calculation of the baseline erosion and the topline erosion was carried out for the study area. The spatial distribution of these values and the age of these surfaces were also analyzed. The elevation and the age of the peneplain have been defined in [An L. D., 1994; Thang N. G., 2007]. Three different levels of the line erosion which coincide with three different levels of the top line erosion have been defined in the study area. The 3<sup>rd</sup> baseline erosion is considered as the local baseline erosion level. The position of the 2<sup>nd</sup> baseline erosion and the 1<sup>st</sup> baseline erosion at the height of 500m - 2000m suggests that the region is activated since the Holocene [Tuyen N. H., 2012a]. The dominant deep erosion level shown on the map of the vertical elevations reflects the tectonic activity. The cutting level on the 3<sup>rd</sup> baseline erosion reflects both the long duration and the large space as

compared to the 2<sup>nd</sup> baseline erosion and the 1<sup>st</sup> baseline erosion. The contour map of the morphological structure and the differentiated intensity was calculated for the negative values of the topline erosion and for the baseline erosion values on the same level. The map reflects the uplift and the subsidence of the relief with respect to the local baseline erosion.

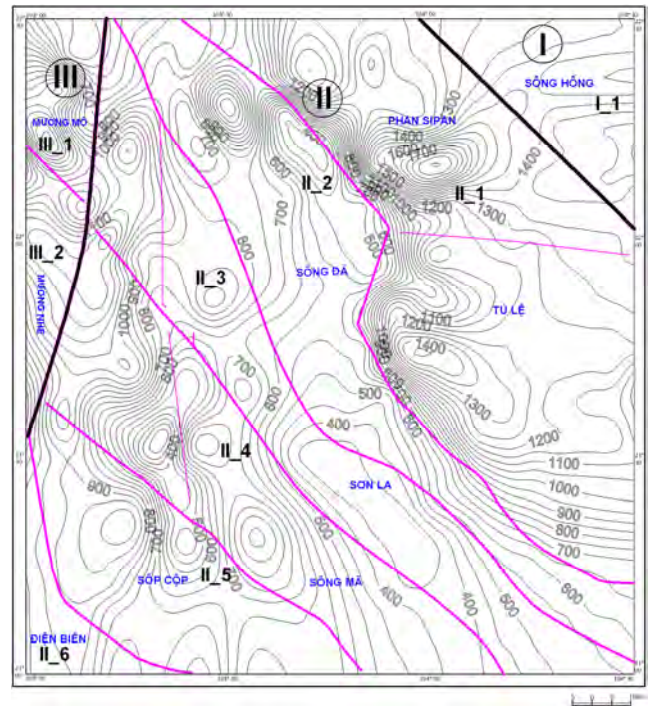


Figure 4a. The counter map of the negative values of the 3<sup>rd</sup> topline erosion - 3<sup>rd</sup> baseline erosion.

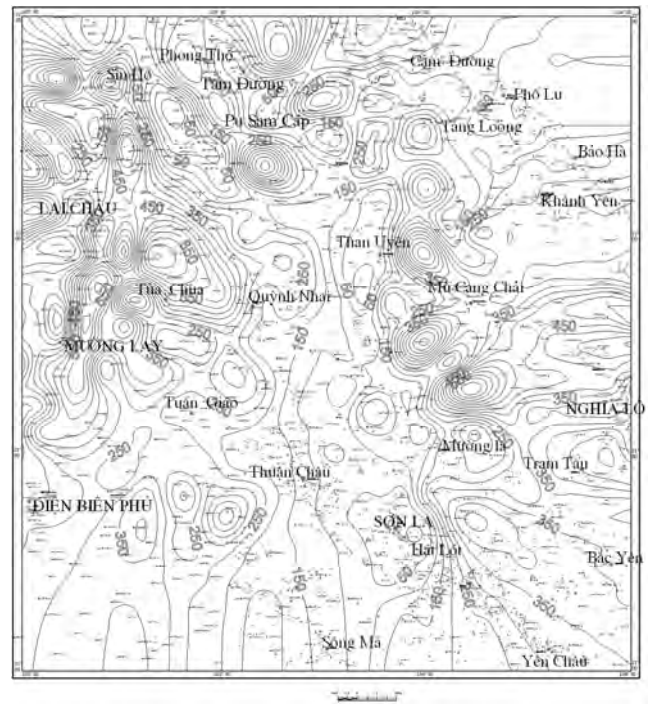


Figure 4b. The counter map of the negative values of the 1<sup>st</sup> topline erosion - 1<sup>st</sup> baseline erosion.

The maps calculated for the negative values of the topline erosion and for the values the baseline erosion on the same level suggest the ongoing vertical movements that form the regional structure and local geological body (figure 4. a and 4. b). These maps allow to divide the study area into geoblocks and to determine the relative movements between them. The maps allow us to estimate the amplitude of the vertical movements of the crust.

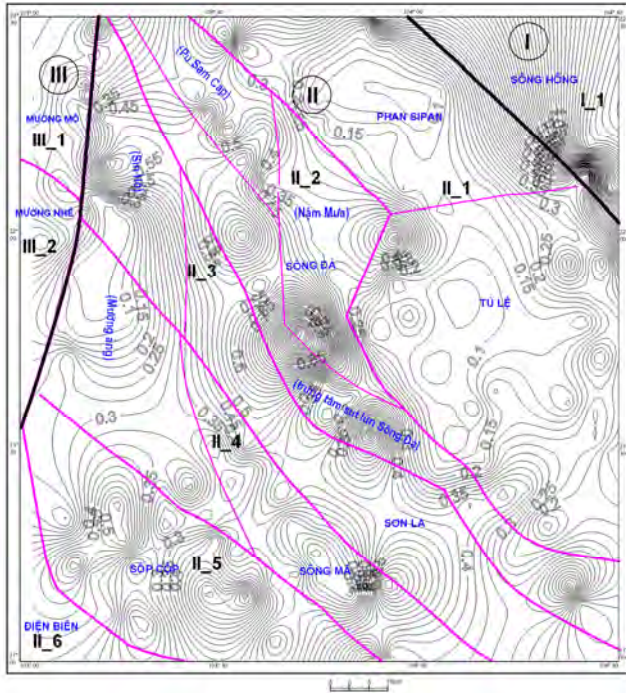


Figure 5a. The counter map of the values of the  $V_j$  index in Tuan the Giao area.

We have also calculated the geomorphologic indexes that have been used for delineating the geoblocks in the Tuan Giao area. Specifically, we have calculated (figure 5. a and 5. b) the sinuosity index ( $S_{mf}$ ) and the index of the correlation ratio ( $V_j$ ) between the bottom width of the valley and the height of the valley [Robert S. Y., 1997]. The Mountain Front Sinuosity is a classic index of the tectonic activity, the values of which are defined with the formula (1):

$$S_{mf} = L_{mf}/L_s \tag{1}$$

where  $S_{mf}$  - Mountain front sinuosity;  $L_{mf}$  - Sinuous length measured along an undulating, weaving path at the mountain hill slope-alluvial fan slope break;

$L_s$ - Straight-line length of the mountain front segment.

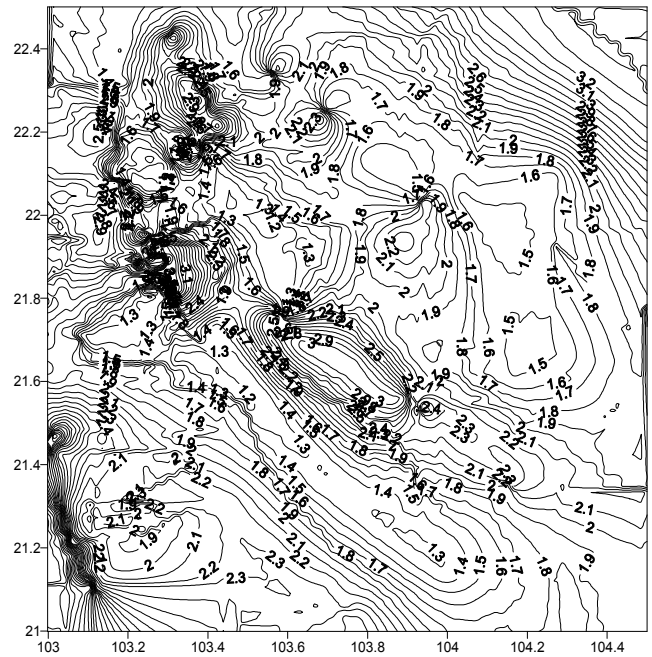


Figure 5b. The values of the  $S_{mf}$  index in the Tuan Giao area.

Therefore, the  $S_{mf}$  index characterizes the activity of faults or boundaries between geoblocks. The smaller values of the  $S_{mf}$  suggest a higher activity of the fault zone and, in turn, the higher values of the  $S_{mf}$  indicate the smaller activity. The results of the calculation show that in the study area the  $S_{mf} \leq 2.0$  is typical for the major faults that form the boundaries of the geoblocks. The values of the  $S_{mf}$  are given in Table 1 for each geoblocks. The smaller values of the  $S_{mf} \leq 2.0$  are typical for the Muong Than - Khanh Yen, Son La, Tuan Giao, Pan Ma geoblock boundaries that suggest their highest activity in the study region (table 1). The values of the  $S_{mf}$  in range of 2.0 - 2.5 indicate the moderate activity of the faults. Such values are characteristic for the Song Ma, Muong La - Bac Yen, Phong Tho, Lai Chau - Dien, Song Da geoblocks boundaries. For the other faults the values of the  $S_{mf} \geq 2.5$  suggest the lesser activity. It should be stressed that along the strike of the fault their individual segments are characterized by different values of  $S_{mf}$  indicating the different rate of the activity of these segments (figure 5c).

Table 1. The  $S_{mf}$  values for the Tuan Giao area.

STT	$S_{mf}$	$L_s$ (km)	$L_{mf}$ (km)	STT	$S_{mf}$	$L_s$ (km)	$L_{mf}$ (km)	STT	$S_{mf}$	$L_s$ (km)	$L_{mf}$ (km)	STT	$S_{mf}$	$L_s$ (km)	$L_{mf}$ (km)
A-1	1.31	22.79	29.84	D-6	1.02	21.13	21.60	G-28	1.24	12.23	15.15	P-24	2.59	11.18	29.00
B-2	2.17	9.69	21.04	D-8	2.50	38.09	95.06	G-29	1.19	6.75	8.04	Q-22	2.00	46.87	93.80
B-3	2.38	5.83	13.89	D-8	2.89	19.82	57.36	G-30	1.24	31.72	39.23	Q-23	4.39	30.92	135.60
B-4	1.33	11.94	15.91	E-10	1.84	12.59	23.22	G-7	1.00	15.58	15.65	Q-24	1.18	11.18	13.21
B-6	2.34	21.13	49.35	E-11	1.12	7.14	8.00	H-13	1.44	22.61	32.51	R-25	4.04	44.68	180.70
C-1	1.26	20.91	26.39	E-12	3.63	15.68	56.89	I-16	2.14	49.00	105.00	S-19	2.60	35.50	92.17
C-2	1.14	9.08	10.38	E-8	1.09	19.82	21.55	K-14	2.67	17.31	46.19	S-31	3.05	48.24	147.00
C-26	3.25	5.49	17.83	E-9	1.25	29.70	37.04	K-15	1.45	34.75	50.46	T-28	1.09	12.23	13.31

STT	Smf	Ls (km)	Lmf (km)	STT	Smf	Ls (km)	Lmf (km)	STT	Smf	Ls (km)	Lmf (km)	STT	Smf	Ls (km)	Lmf (km)
C-27	3.06	28.41	86.87	F-11	1.25	13.82	17.30	M-17	2.40	16.50	39.60	T-29	3.94	6.75	26.58
C-3	1.10	5.83	6.40	F-9	1.48	29.70	44.10	M-18	1.94	35.23	68.36	T-30	2.48	31.72	78.56
C-4	1.29	11.94	15.43	G-10	1.04	12.59	13.12	M-19	2.31	35.50	82.16	T-31	4.35	48.24	210.00
C-5	1.01	13.57	13.74	G-12	1.33	15.68	20.79	M-20	1.93	46.39	89.47	U-20	3.29	46.39	152.40
C-7	1.08	15.58	16.86	G-26	1.28	5.49	7.04	N-21	2.60	44.62	116.10	P-24	2.59	11.18	29.00
D-11	1.92	21.96	42.25	D-6	1.02	21.13	21.60	P-22	2.26	46.87	105.70	Q-22	2.00	46.87	93.80
								P-23	2.47	30.92	76.48	Q-23	4.39	30.92	135.60

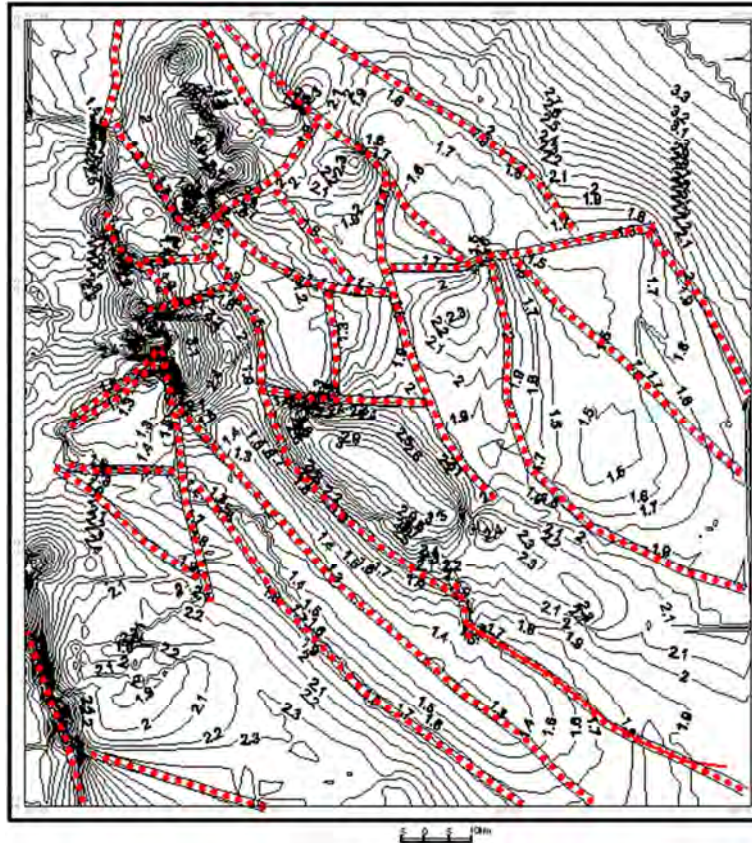


Figure 5c. The counter map of the  $S_{mf}$  indicator and the active fault segment (red dot line).

The  $V_f$  geomorphic indicator is fruitful parameter to identify the activated area. The indicator is defined with the formula (2):

$$V_f = 2V_{fw} / [(E_{ld} - E_{sc}) + (E_{rd} - E_{sc})] \quad (2)$$

where:  $V_{fw}$ - the width of the valley bottom;  $E_{sc}$ - the elevation of the valley bottom

$E_{ld}$  - elevations of the left valley divides;  $E_{rd}$  - elevations of the right valley divides

The values of  $V_f < 0.4$  suggest the increasing uplift rates, while the values of  $V_f$  in range of  $0.4 - 0.6$  indicate the moderate uplift and the values of  $V_f > 0.6$  are characteristic for the areas of the low uplift.

The values of  $V_f$  defined within the entire study area (figure 5) allow us to distinguish the geoblocks in accordance with their uplift rate (table 2). The highest uplift is characterized by  $V_f < 0.4$ , the average one when  $V_f = 0.4 - 0.6$ , and a weaker one is if  $V_f > 0.6$ . Figure 5 shows that geoblocks clearly differ from each other in the uplift rate.

The studies of active tectonics [Edward A. E., 1996]

demonstrated that the last orogenic processes started in the Oligocene have formed the regional planation surfaces in the Paleocene [An L. D 1994, Thang N. G, 2007, 2009, Thuy N. N, 2005]. The Pliocene - Quaternary (about 5 million year) orogenic phase affected the Northwest region of Vietnam is evidenced in the elevation of the relief. The present mountainous topography in Northwest of Vietnam have been resulted from the elevated surfaces deformed during the last 5 million years [Tuyen N. H., 2012a]. The most elevated and deformed surfaces with the elevation amplitude of 1.3 km to 4.0 km were observed in the Hoang Lien Son. In the southwest the amplitude is gradually decreased up to 1.5 km in the Song Da - Son La In the northwest the largest amplitude of 3,3 km were observed in the Pu Sam Cap.

The rate of the average vertical movements ( $V_{tb}$ ) for the Pliocene - Quaternary time was calculated for the entire region using the method proposed by Tuyen N. H [2012a]. The 2<sup>nd</sup> geoblocks remarkably differ in the  $V_{tb}$  values (figure 6a).

*Earth's Crust Thickness and the Horizontal Movements:*

The principles for evaluating variations of the Earth's crust thickness (*horizontal stress pattern*) have been overviewed by Cao D. T. [2005]. The stress on the crust layers is formed mainly due to the residual deformation in the asthenosphere layers. The method has been developed and applied to the Vietnam territory [Cao D. T., 2005, 2008; Tuyen N. H; 2012a]. According to this study, the Tuan Giao area is a rather complicated but fairly stable in each local

structural unit, which is characterized by the direction and magnitude of the horizontal displacements. We have applied the most recent data on the deep structure and gravity to determine the Earth's thickness in the Tuan Giao Area [Hai D. T., 2003; Thuy N. N 2005; Tuyen N. H, 2010]. To study the pattern of crustal horizontal movement, firstly the diagram of the Earth's thickness changes in the study area should be defined.

Table 2. The  $V_f$  values the Tuan Giao area.

STT	Vfw (m)	Eld (m)	Erd (m)	Esc (m)	Vf	STT	Vfw (m)	Eld (m)	Erd (m)	Esc (m)	Vf	STT	Vfw (m)	Eld (m)	Erd (m)	Esc (m)	Vf
SH12	90	1000	1062	90	0,095643	DB06	400	1852	1700	200	0,253807	DB22	200	1000	1800	280	0,178571
SH13	110	1070	1100	470	0,178862	DB07	200	1500	1981	200	0,129828	DB23	200	1410	1500	280	0,170213
SH14	200	1120	2030	260	0,152091	DB08	100	644	1100	180	0,144509	DB24	300	700	1300	276	0,414365
SH15	150	1310	1400	200	0,12987	DB09	300	1200	1300	470	0,384615	DB25	120	1400	880	400	0,162162
SH16	170	2410	2240	1660	0,255639	DB10	200	1230	1050	400	0,27027	DB12	300	1100	2178	400	0,242131
SH17	100	1340	1300	800	0,192308	DB11	100	1170	1300	400	0,11976	DB13	100	1050	1540	340	0,104712
SH18	300	1140	800	300	0,447761	DB12	300	1100	2178	400	0,242131	DB14	70	1500	1400	480	0,072165
SH19	100	1800	1100	500	0,105263	DB21	150	1500	1900	290	0,106383	DB15	300	1300	1420	200	0,258621
SH20	300	1700	1140	180	0,241935	DB22	200	1000	1800	280	0,178571	DB16	50	1410	110	200	0,089286
SH21	100	931	720	80	0,134138	DB23	200	1410	1500	280	0,170213	DB17	70	1800	1500	200	0,048276
SH22	80	1830	1200	280	0,064777	DB25	120	1400	880	400	0,162162	DB18	80	1000	700	200	0,123077
SH23	150	700	920	380	0,348837	DB13	100	1050	1540	340	0,104712	DB19	250	570	1520	200	0,295858
SH24	80	1200	900	280	0,103896	DB14	70	1500	1400	480	0,072165	DB20	350	1200	1600	300	0,318182
SH25	100	830	950	80	0,123457	DB15	300	1300	1420	200	0,258621	DB26	80	1050	1000	290	0,108844
SH26	150	1000	1120	470	0,254237	DB16	50	1410	110	200	0,089286	DB27	100	1100	1130	290	0,121212
DB01	200	1360	2019	500	0,168138	DB17	70	1800	1500	200	0,048276	DB28	80	1600	1600	300	0,061538
DB02	250	700	1300	290	0,352113	DB18	80	1000	700	200	0,123077	DB29	70	700	1600	300	0,082353
DB03	150	1700	1720	493	0,123254	DB19	250	570	1520	200	0,295858	DB30	150	1730	1100	290	0,133333
DB04	300	1630	1250	350	0,275229	DB20	350	1200	1600	300	0,318182	DB31	250	1100	1300	380	0,304878
DB05	200	1100	800	294	0,304878	DB21	150	1500	1900	290	0,106383	DB32	80	1200	1120	500	0,121212
												DB33	80	1200	1240	500	0,111111

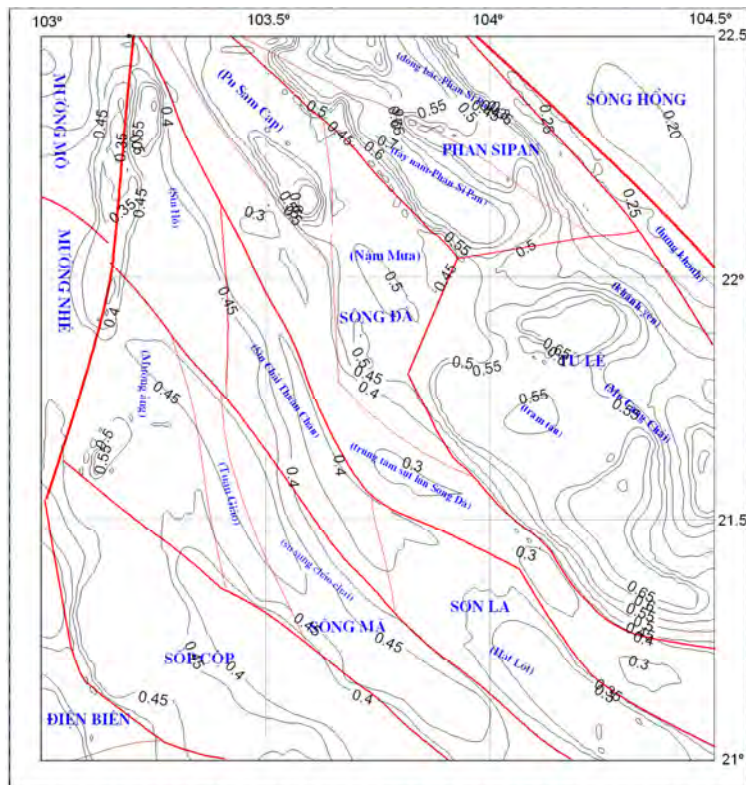


Figure 6a. The elevation in the Plio-Quaternary.



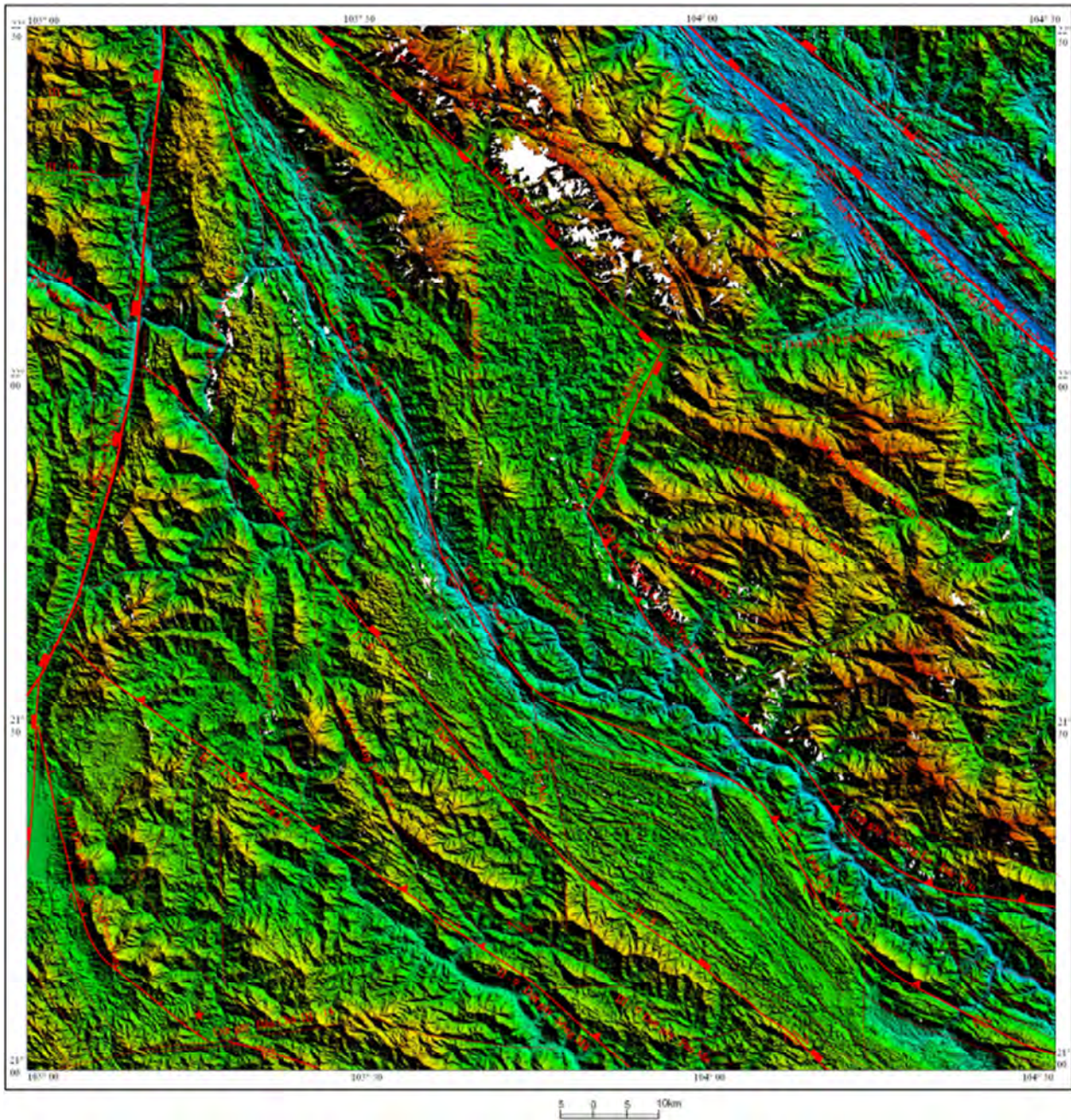


Figure 7b. The Digital Elevation Modal (DEM).

### 2.3. The Sketch of the Geoblocks of the Tuan Giao Area

The final goal in studying the active geoblocks is the construction of the geodynamic map of the region. The map introduces the system of geoblocks and their major characteristics, including:

- the system of the geoblocks, the network of their boundaries and loci of the nodes;
- ranks and kinematics of the block boundaries;
- the difference in the structure of each geoblock;
- the amplitude of the vertical movement in the Pliocene - Quaternary and evidences of the horizontal displacements;

- the bodies of magmatic intrusion and extrusion;
- the deformation rate during the Pliocene - Quaternary period;
- the intensity of the geomorphologic processes characterized by the  $S_{mf}$  and  $V_f$  indicators;

The final results have been obtained through the analysis of different data which allow delineating the sketch of the geoblocks and determining their parameters. The compiled geoblock sketch shows four the 2<sup>nd</sup> geoblocks. They are the Hoang Lien Son, Song Da - Son La, Song Ma, Song Ma - Sop Cop, and Dien Bien geoblocks. These 2<sup>nd</sup> geoblocks are a part of the Northwest Vietnam first order geoblock, that borders the first order geoblocks of Muong Te and Northeast Vietnam along the large Lai Chau- Dien Bien and Red River faults (figure 8).



classify all intersections into seismogenic and non-seismogenic ones with respect to  $M_s = 5.0$ .

**3.1. Methodology of Recognition Earthquake Prone Areas (EPA)**

The EPA methodology in every detail is described by Gorshkov et al. [2003]. It was firstly introduced by Gelfand et al. [1972] and then within 40 years has been applied to many seismic regions of the world for identifying earthquake prone areas for strong events of different target magnitudes [Cisternas et al. 1985; Gelfand et al., 1976; Gorshkov et al. 2000, 2002, 2003, 2004, 2009, 2010; Gvishiani et al., 1987, 1988]. After the publication of the results of the recognition most of the studied regions have been affected by target earthquakes which proved the reliability of the methodology. Most recently Soloviev et al. [2014] has shown that 87% of the post-publication events with target magnitudes occurred at the nodes that were recognized in advance prone to such size earthquakes.

The North Vietnam territory has been recently studied with the EPA methodology by Tuyen N. H et al. [2012b]. In this work, we apply pattern recognition technique to define seismogenic nodes prone to  $M5+$  in the Tuan Giao area.

The set of the nodes delineated with the GD model in the Tuan Giao area includes 70 nodes (figure 9). The recognition enables to divide them into two classes, namely, (1) class D, which includes the nodes where earthquakes with  $M_s5+$  may occur, and (2) class N, containing the nodes where only

earthquakes with  $M_s < 5.0$  may happen.

To apply the CORA-3 algorithm, all objects of recognition (nodes) should be characterized by uniform set of parameters relevant to seismicity. In this work, we employ 17 parameters enumerated in Table 3. Most of them, apart from the parameters related to the magnetic anomalies, have been previously employed for the EPA recognition [see the review of this problem by Gorshkov et al. 2003]. In this work we define the node as the circle of 20 km in radius. Such dimension of the node is consistent with the earthquake source. The actual values of the parameters listed in Table 3 have been defined for each node inside the circle of 20 km in radius from topographic, geological, gravity, and magnetic maps as well as from the GB map (figure 9).

The CORA-3 algorithm operates in a binary vector space [Gelfand et al., 1976; Gorshkov et al., 2003] Therefore, the actual values of the parameters were transformed into binary vectors by discretization and coding with the CODM software [Soloviev, 1991]. During discretization the range of the actual values of each parameter was divided into two (“small” and “large”) or three (“small”, “medium”, and “large”) intervals. The thresholds of the discretization discriminating the “small” values from “medium” and” large ones are given in Table 3. Consequently, each node is represented by a binary vector of values of the parameters. The set of these vectors is the input for the PRAL software [Soloviev, 1991] realizing the CORA-3 algorithm.

*Table 3. Parameters used for recognition and thresholds of their discretization.*

<b>A) Topographic parameters</b>	
1. Maximum topographic altitude, m (Hmax)	1394m; 1666m
2. Minimum topographic altitude, m (Hmin)	202m; 456m
3. Relief energy, m ( $\Delta H$ ) (Hmax - Hmin)	1167m
4. Distance between the points Hmax and Hmin, km (L)	8km
5. Slope, ( $\Delta H/L$ )	155
6. Morphological parameter (Mor), this parameter is equal to one of the following six values in accord with the morphology within each node:	
i1 - mountain and plain (m/p)	i2 - mountain and piedmont (m/pd)
i3 - mountain and mountain (m/m)	i4 - piedmont and plain (pd/p)
i5 - piedmont only (pd)	i6 - plain only (p)
<b>B) Parameters from the GB map</b>	
7. The highest rank of the boundary in a node, (HR)	1 <sup>st</sup> or 2nd
8. Number of boundaries forming a node, (NL)	2
9. Distance to the nearest 1st rank boundary, km, (D1)	25km; 53km
10. Distance to the nearest 2nd rank boundary, km, (D2)	3km
11. Distance to the nearest node, km, (Dn)	13km
<b>C) Gravity and magnetic parameters</b>	
12. Maximum value of Bouguer anomaly, mGal, (Bmax)	-90mGal
13. Minimum value of Bouguer anomaly, mGal, (Bmin)	-102mGal
14. Difference between Bmax and Bmin, mGal, ( $\Delta B$ )	16mGal
15. Maximum value of magnetic anomaly, nT, (Mmax)	-110nT
16. Minimum value of magnetic anomaly, nT, (Mmin)	-170nT
17. Difference between Mmax and Mmin, nT, ( $\Delta M$ )	60nT

Application of the CORA-3 algorithm includes the learning and classification stages [Gelfand et al., 1976; Gvishiani et al., 1988; Gorshkov et al., 2003]. At the learning stage the algorithm selects distinctive features that are characteristic for each class on the basis of the training set presented by  $D_0$  and  $N_0$  subsets. These subsets include the

sample nodes representative of the classes D and N, respectively. At the classification stage the algorithm defines the class to which each node belongs by counting numbers of the D- and N characteristic features that each node possesses and assigns each node to one of the two classes in accordance with the number of prevailing features.

**3.2. Results of the Recognition for the Tuan Giao Area**

The GB model delineated 70 nodes in the Tuan Giao area (figure 9). They were *apriori* divided into three sets for the learning stage of the recognition using the information on earthquakes recorded in the Tuan Giao area. The spatial distribution of earthquakes with  $M_s \geq 4.0$  is shown in figure 9.

Since we classify nodes with respect to the threshold of magnitude  $M_s = 5.0$ , it is necessary to select the sample nodes where events of the equal or exceeding magnitudes have already taken place. Therefore in the subset  $D_0$ , we

included eight nodes 3, 4, 5, 7, 14, 17, 43, and 67 that are situated most closely to the epicenters of earthquakes with  $M \geq 5.0$  (figure 9). The nodes that are most distant from the epicenters of  $M5+$  were assigned to the set  $N_0$ . Four nodes 1, 8, 9, and 68 where there are smaller earthquakes with  $4.0 \leq M_s < 5.0$  we included in the subset X. The nodes from the subset X are not employed at the learning stage for selecting characteristic features of D and N classes. But their belonging to one of these classes was defined at the classification stage.

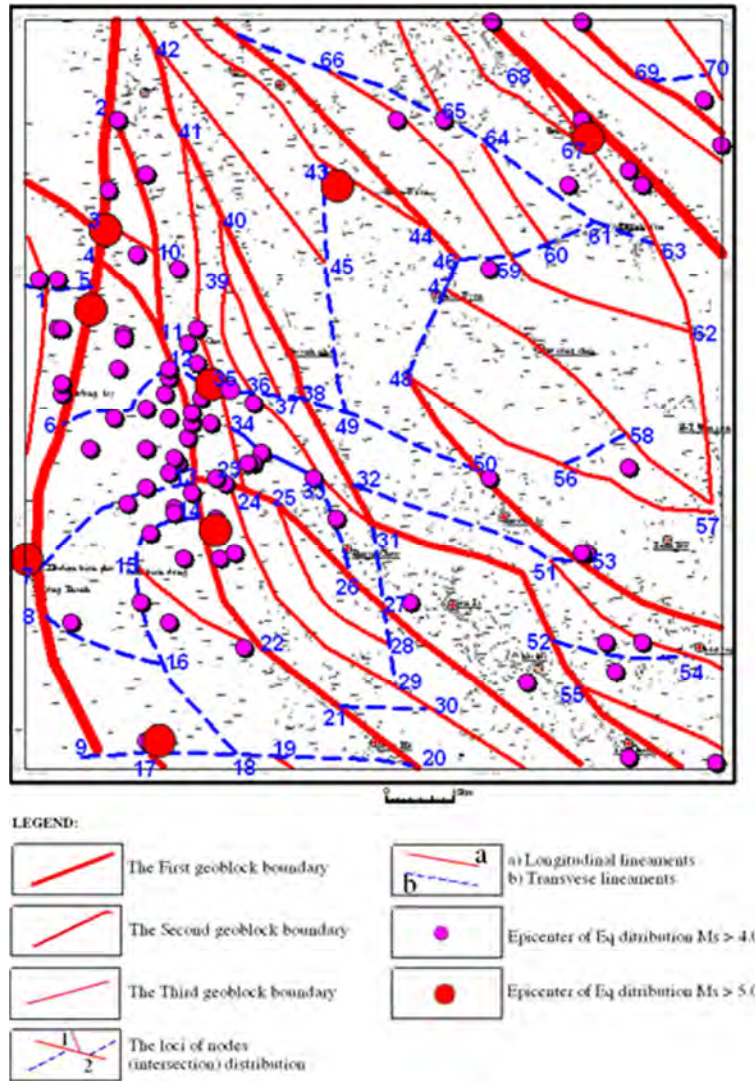


**Figure 9.** The GB map of the Tuan Giao area and seismicity.

The nodes have been classified in accordance with the decision rule defined by the CORA-3 algorithm at the learning stage. The decision rule includes eight D - and ten N characteristic features formed by the following parameters:  $H_{min}$ ,  $H_{max}$ ,  $L$ ,  $dH$ ,  $dH/L$ ,  $D1$ ,  $D2$ ,  $Dn$ ,  $B_{max}$ ,  $B_{min}$ ,  $M_{max}$ ,  $M_{min}$ ,  $dM$ . It was found that seismogenic nodes are characterized by the “large” values of  $dH$  and  $dH/L$  which indicate the contrast and high rate of the vertical tectonic movements around the nodes recognized prone to  $M5+$ . Additionally, the “small” values  $D1$ ,  $D2$ , and  $Dn$

characteristic for D nodes suggest the increased fracturing of the crust in the vicinity of such nodes and the importance of the 1<sup>st</sup> and 2<sup>nd</sup> rank geoblock’s boundaries in the spatial control of seismogenic nodes. Besides, the large negative values of the gravity and magnetic anomalies are typical for D nodes.

As a result we have recognized 15 seismogenic nodes prone to  $M_s \geq 5.0$  including all eight nodes from the initial subset  $D_0$ , four nodes (10, 11, 12, 69) from  $N_0$ , and three nodes (1, 8, 9) from the subset X. These nodes are shown in

figure 10. Within seven of the recognized D nodes (1, 8, 9, 10, 11, 12, 69) earthquakes of the target size (Ms5+) are not recorded till present (figure 10).

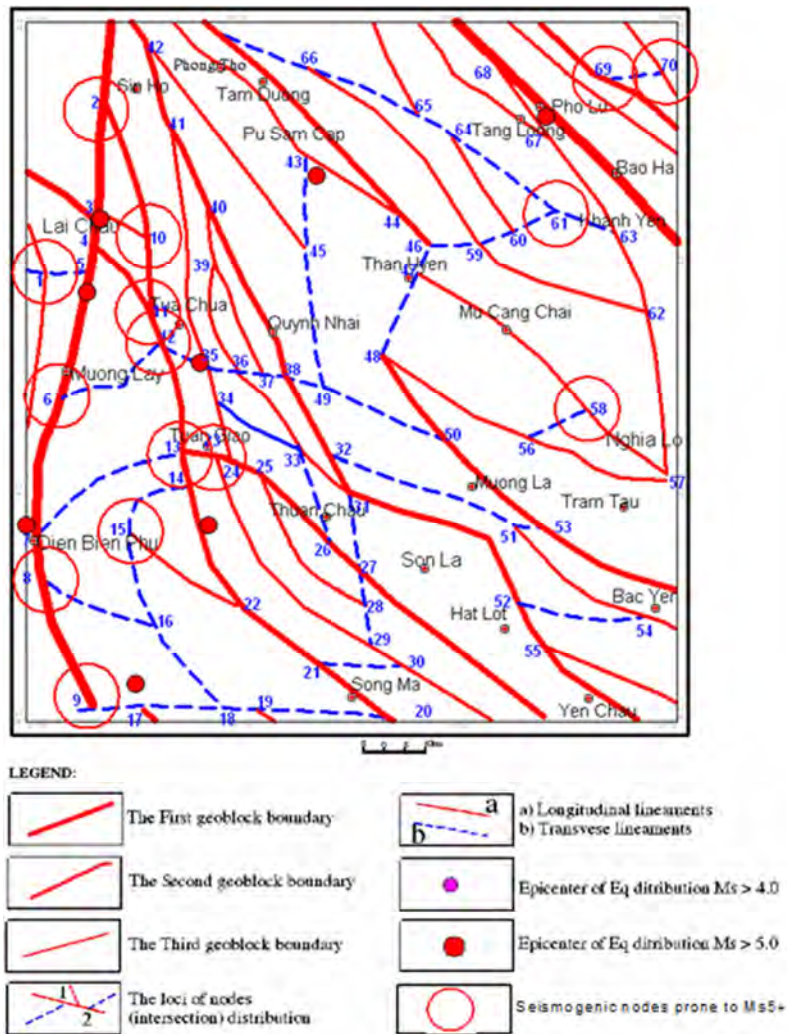


Figure 10. The sketch of the predicted seismogenic nodes in the Tuan Giao area.

### 4. Conclusions

The joint analysis of geological, geophysical, and geomorphological data allowed identifying the geoblocks sketch of the Tuan Giao area that shows the hierarchical system of the geoblocks and their characteristics of the recent tectonic activity. Totally four largest geoblocks of the second rank have been delineated. They are the the Hoang Lien Son, Son La - Song Da, Song Ma - Sop Cop and Dien Bien geoblocks. These the 2<sup>nd</sup> rank geoblocks continuously were divided into the smaller sub-blocks separated by the inner-boundary system. The 2<sup>nd</sup> rank geoblocks exhibit different rate of the vertical movements during the Pliocene - Quaternary time. In the Hoang Lien Son geoblock the rate of the vertical movements is 0.6 - 0.9 mm/year, in the Son La – Song Da geoblock the rate is 0.1 - 0.7 mm/year, in the Song Ma - Sop Cop geoblock the rate is 0.3 - 0.6 mm/ year, and in the Dien Bien geoblock the rate is 0.1 - 0.3 mm / year.

The study demonstrates that the pattern recognition approach to identify earthquake prone areas is applicable to

the Tuan Giao region in Northwest Vietnam that is characterized by a complex and heterogeneous tectonic structure and topography. The recognition performed provides the essential information for the improvement of the seismic hazard assessment for the study region. A number of seismogenic nodes have been recognized in the areas where events with M5+ have not been recorded up to now. The results of this work can be improved in the further studies through testing more wide range of geomorphic and geophysical parameters of the nodes for their classification into seismogenic and non-seismogenic ones.

Acknowledgements: This study completed under support from Institute of Geophysics, Vietnam Academy of Science & Technology (VAST) - project code VAST. HTQT. NGA.08/15-16. The part of research conducted in frame of the “Joint Vietnam-Russia Joint Laboratory for Marine Geosciences” (IMGG VAST – POI FEB RAS), partially supported by the joint FEB RAS – VAST Project 16-005 “Investigation of the deep fluid dynamics features and degassing processes of the lithosphere in the transition zone

from continent to the Gulf of BacBo by geophysical and gasgeochemical methods”.

The authors would like to thank for the useful comments

Assoc. Prof. Dr. Cao Dinh Trieu of IGP, VAST and Assoc. Prof. Dr. Chu Van Ngoi from University of Science, VNU.

**Table 4.** The inputted 18 parameters of “nodes” for recognition of prone areas of Earthquake with  $M > 5.0$  for Tuan Giao by CORA3.

STT (1)	Hmax (2)	Hmin (3)	L (4)	$\Delta H$ (5)	dH/L (6)	HR (7)	Q (8)	NL (9)	D1 (10)
V_1	1398	416.5	08.5	0981	115.44	3	00.12	2	10.20
V_2	1809	224	04.5	1585	352.17	1	00.70	2	00.00
V_3	1544	173.8	08.6	1370	159.84	1	01.20	3	00.00
V_4	1500	187.6	06.6	1312	198.48	1	05.00	2	00.00
V_5	1664	207	03.6	1457	404.76	1	00.10	2	00.00
V_6	1275	347.9	03.9	0927	237.67	1	10.00	2	00.00
V_7	1140	474	11.0	0666	060.59	1	08.10	2	00.00
V_8	1507	468.6	06.5	1038	159.70	1	16.00	2	00.00
V_9	1450	629.6	08.0	0820	102.15	1	13.00	2	00.00
V_10	1621	161.8	06.5	1459	224.44	2	00.40	2	12.80
V_11	1518	229.2	08.0	1289	160.26	2	00.10	2	16.40
V_12	1570	253.7	03.8	1316	346.35	2	00.10	3	21.30
V_13	1579	488.3	13.0	1091	083.91	2	00.10	3	33.50
V_14	1843	483.7	08.2	1359	165.12	2	00.10	2	36.20
V_15	1656	569.7	08.1	1087	133.65	3	00.10	2	22.40
V_16	1360	456.5	10.2	0903	088.48	3	02.00	2	24.80
V_17	1416	588.3	08.5	0828	097.95	2	00.36	2	12.20
V_18	1712	846.9	11.2	0865	077.28	3	00.80	2	31.00
V_19	1750	848.6	10.0	0902	090.61	3	00.50	2	38.90
V_20	1313	310.3	08.3	1002	120.31	2	01.50	2	70.50
V_21	1305	390.1	03.4	0915	267.53	2	00.37	2	57.50
V_22	1411	368.3	03.5	1043	297.90	2	00.13	2	45.20
V_23	1593	554	06.4	1039	162.84	2	00.10	2	41.80
V_24	1631	558.2	08.1	1073	132.18	2	00.72	2	45.50
V_25	1666	618.8	04.3	1047	243.54	2	00.15	2	53.20
V_26	1467	542.8	10.1	0925	091.35	2	12.30	2	68.30
V_27	1311	525.5	03.8	0786	206.79	2	05.70	2	76.50
V_28	1781	469	11.3	1312	116.08	3	05.80	2	75.70
V_29	1789	449.2	15.4	1340	087.22	3	03.70	2	75.00
V_30	1755	531.8	06.0	1223	203.80	3	01.60	2	79.20
V_31	923.4	208.8	08.2	0715	087.04	2	03.30	3	74.10
V_32	993.3	159.2	09.1	0834	092.17	2	00.10	2	69.20
V_33	1205	147.1	13.1	1058	080.98	3	06.70	3	69.40
V_34	1653	433	12.6	1220	096.79	3	01.50	2	37.90
V_35	1319	333.2	08.7	0986	113.04	3	09.70	3	33.00
V_36	1500	373.6	07.2	1126	156.46	3	08.20	2	40.40
V_37	1524	131.2	10.6	1393	131.16	3	11.60	2	46.00
V_38	1182	130.8	12.7	1051	082.55	2	01.20	2	52.10
V_39	1768	137	09.4	1631	172.75	3	09.30	2	29.40
V_40	1135	145.3	09.3	0989	106.85	2	25.00	2	26.10
V_41	1426	202.8	12.5	1223	098.27	2	80.00	2	17.60
V_42	1719	307.9	09.1	1411	154.76	2	89.00	2	09.30
V_43	2420	503.4	12.2	1916	156.57	3	70.00	2	49.70
V_44	2016	494.1	06.7	1522	227.18	2	32.00	2	61.30
V_45	1292	437.5	03.0	0855	285.84	3	48.00	2	51.00
V_46	2055	520	07.0	1535	219.27	2	92.00	3	56.70
V_47	2071	467.1	13.9	1604	115.38	3	95.00	2	65.20
V_48	1652	329.3	05.2	1323	256.83	2	95.00	3	73.00
V_49	786.9	121.9	12.3	0665	053.89	3	97.00	2	60.80
V_50	1674	131.6	07.4	1542	209.80	2	53.00	2	71.70
V_51	1422	118.3	07.7	1304	169.33	3	72.00	3	74.30
V_52	1138	259.1	05.4	0879	162.83	2	00.10	2	84.00
V_53	2133	116	08.1	2017	249.01	2	00.12	2	72.00
V_54	1756	116.9	09.5	1639	172.55	3	00.15	2	68.00
V_55	1547	379.6	09.0	1167	129.69	2	00.94	2	85.00
V_56	2408	869.2	12.6	1539	122.10	3	00.95	2	57.90
V_57	1435	307.3	07.1	1127	157.91	3	01.08	3	43.40
V_58	2329	1022	07.4	1307	176.61	3	00.58	2	42.50
V_59	1937	403	07.2	1534	213.12	3	00.94	2	34.30
V_60	1394	212.9	08.1	1181	145.79	3	01.52	2	26.00
V_61	1234	159.1	05.3	1075	202.90	3	03.00	2	16.00

STT (1)	Hmax (2)	Hmin (3)	L (4)	ΔH (5)	dH/L (6)	HR (7)	Q (8)	NL (9)	D1 (10)
V_62	1339	128.2	13.7	1210	088.34	3	05.20	2	17.00
V_63	909.2	125.2	08.6	0784	091.17	3	00.72	2	09.20
V_64	1733	186.2	10.5	1547	147.30	3	01.10	2	20.00
V_65	2415	693.1	13.3	1722	129.47	3	00.65	2	21.50
V_66	2883	770	11.4	2113	185.39	3	00.12	2	33.00
V_67	465	59	11.6	0406	035.00	3	00.94	2	06.00
V_68	466.5	64	09.5	0403	042.37	1	01.08	2	00.00
V_69	1229	100.4	09.2	1128	122.64	2	00.14	2	15.00
V_70	1146	151	05.3	0995	187.76	3	00.12	2	25.50

Table 4. Continue.

STT (1)	D2 (11)	Dn (12)	Bmax (13)	Bmin (14)	ΔB (15)	Mmax (16)	Mmin (17)	ΔM (18)	Mor (19)	Latitude (20)	
										x	y
V_1	20.10	10.40	-90	-112	022	-250	-310	060	3	103.161	22.088
V_2	00.00	18.50	-90	-112	022	-150	-290	140	3	103.157	22.021
V_3	00.00	06.70	-108	-116	008	-250	-290	040	3	103.142	21.965
V_4	00.00	06.70	-108	-124	016	-230	-290	060	3	103.076	21.688
V_5	00.00	06.70	-100	-118	018	-230	-300	070	3	103.027	21.400
V_6	28.30	28.60	-90	-110	020	-260	-300	040	3	103.032	21.305
V_7	39.40	10.40	-92	-100	008	-270	-300	030	1	103.159	21.026
V_8	42.10	10.40	-98	-108	010	-260	-290	030	1	103.281	22.033
V_9	11.20	11.80	-98	-102	004	-260	-280	020	3	103.289	21.869
V_10	00.00	13.00	-98	-104	006	-250	-270	020	3	103.311	21.808
V_11	00.00	09.20	-92	-108	016	-210	-260	050	3	103.359	21.576
V_12	00.00	09.20	-92	-110	018	-200	-240	040	3	103.375	21.507
V_13	00.00	07.20	-96	-104	008	-170	-230	060	3	103.235	21.404
V_14	00.00	07.20	-96	-102	006	-180	-230	050	3	103.292	21.211
V_15	16.90	17.50	-96	-104	008	-220	-250	030	3	103.265	21.033
V_16	18.60	20.90	-98	114	-212	-210	-250	040	3	103.452	21.032
V_17	00.00	11.80	-98	-104	006	-210	-250	040	3	103.529	21.029
V_18	32.20	09.20	-100	-106	006	30	-190	220	3	103.832	21.010
V_19	27.30	09.20	-92	-100	008	10	-130	140	3	103.675	21.124
V_20	00.00	12.30	-60	-84	024	120	-50	170	3	103.491	21.249
V_21	00.00	12.90	-76	-94	018	-70	-130	060	3	103.437	21.566
V_22	00.00	21.20	-76	-112	036	-80	-200	120	3	103.474	21.557
V_23	00.00	03.50	-96	-100	004	-160	-190	030	3	103.538	21.537
V_24	00.00	03.50	-90	-100	010	-150	-180	030	3	103.693	21.385
V_25	00.00	08.00	-88	-94	006	-100	-160	060	3	103.773	21.324
V_26	00.00	10.60	-80	-94	014	-30	-120	090	3	103.780	21.253
V_27	00.00	07.80	-86	-92	006	-20	-80	060	3	103.795	21.163
V_28	07.00	07.80	-72	-94	022	0	-70	070	3	103.867	21.123
V_29	19.00	09.30	-72	-90	018	-20	-80	060	3	103.748	21.491
V_30	10.00	09.30	-72	-84	012	100	-60	160	3	103.702	21.570
V_31	00.00	09.50	-80	-84	004	-30	-140	110	3	103.633	21.577
V_32	00.00	08.50	-78	-92	014	-50	-160	110	3	103.439	21.682
V_33	05.00	08.50	-82	-102	020	-90	-160	070	3	103.416	21.765
V_34	09.00	09.00	-92	-102	010	-110	-170	060	3	103.486	21.753
V_35	08.50	08.00	-88	-112	024	-110	-210	100	2	103.545	21.747
V_36	10.00	06.10	-90	-102	012	-110	-170	060	3	103.598	21.739
V_37	05.20	06.10	-90	-106	016	-110	-170	060	3	103.431	21.975
V_38	00.00	06.10	-92	-106	014	-110	-150	040	3	103.418	22.096
V_39	05.70	14.40	-84	-92	008	-70	-200	130	3	103.341	22.262
V_40	00.00	14.40	-84	-92	008	-170	-160	-010	3	103.275	22.455
V_41	00.00	22.50	-86	-102	016	-130	-240	110	3	103.644	22.215
V_42	00.00	22.50	-94	-108	014	-70	-160	090	3	103.851	22.095
V_43	06.70	21.80	-102	-126	024	-120	-160	040	3	103.642	22.021
V_44	00.00	10.90	-96	-118	022	-10	-130	120	3	103.927	22.024
V_45	16.30	22.70	-84	-96	012	-100	-180	080	3	103.904	21.962
V_46	00.00	08.10	-98	-124	026	-10	-150	140	3	103.825	21.778
V_47	07.30	08.10	-100	-128	028	-90	-110	020	3	103.969	21.603
V_48	00.00	16.30	-82	-112	030	140	-90	230	3	104.132	21.412
V_49	06.20	09.50	-88	-104	016	-80	-140	060	2	104.129	21.259
V_50	00.00	19.70	-88	-96	008	230	10	220	2	104.187	21.416
V_51	03.30	07.00	-70	-84	014	270	30	240	3	104.425	21.230
V_52	00.00	12.80	-60	-84	024	90	-50	140	3	104.430	21.226
V_53	00.00	07.00	-72	-98	026	290	-90	380	3	104.197	21.159

STT (1)	D2 (11)	Dn (12)	Bmax (13)	Bmin (14)	$\Delta B$ (15)	Mmax (16)	Mmin (17)	$\Delta M$ (18)	Mor (19)	Latitude (20)	
										x	y
V_54	07.80	25.10	-50	-86	036	410	50	360	3	104.163	21.605
V_55	00.00	12.80	-60	-76	016	30	-30	060	3	104.477	21.521
V_56	14.20	15.00	-58	-84	026	90	-330	420	3	104.288	21.670
V_57	25.40	25.60	-88	-116	028	-50	-200	150	3	104.046	22.028
V_58	28.60	15.00	-68	-108	040	-250	-320	070	3	104.122	22.057
V_59	11.00	09.50	-104	-126	022	-70	-170	100	3	104.217	22.099
V_60	20.00	09.50	-94	-118	024	-140	-190	050	3	104.434	21.876
V_61	30.80	10.70	-74	-98	024	-120	-180	060	2	104.357	22.052
V_62	53.80	21.70	-60	-92	032	-110	-190	080	2	103.982	22.255
V_63	43.60	14.40	-60	-88	028	-130	-160	030	3	103.900	22.306
V_64	21.10	10.20	-90	-120	030	40	-110	150	3	103.649	22.402
V_65	19.20	10.20	-96	-124	028	60	-40	100	3	104.204	22.251
V_66	08.00	21.70	-102	-130	028	-100	-160	060	3	104.075	22.411
V_67	19.00	22.60	-62	-88	026	-110	-150	040	2	104.339	22.380
V_68	13.40	22.60	-60	-80	020	-60	-120	060	2	104.464	22.392
V_69	00.00	14.20	-60	-74	014	-130	-160	030	2	103.161	22.088
V_70	07.70	14.20	-56	-86	030	-110	-150	040	2	103.157	22.021

Legend: (1)- The number of nodes; (2)- Maximum topographic altitude; (3)- Minimum topographic altitude; (4)-Relief energy; (5)- Distance between the points Hmax and Hmin; (6) Slope; (7)The % portion of the node area covered by soft (quaternary) sediments; (8)-Morphological parameter; (9)- Highest rank of lineament in a node; (10)- Number of lineaments forming a node; (11)- Distance to the nearest 1st rank lineament; (12)- Distance to the nearest 2nd rank lineament; (13)- Distance to the nearest node; (14)- Maximum value of Bouguer anomaly; (15)- Minimum value of Bouguer anomaly; (16) - Difference between Bmax and Bmin; (17)- Maximum value of magnetic anomaly; (18)-Minimum value of magnetic anomaly; (19)- Difference between Mmax and Mmin; (20)- Latitude of node epicenter.

## References

- [1] Alexeevskaya MA, Gabrielov AM, Gvishiani AD, Gelfand IM, Rantsamn EYa (1977). Formal morphostructural zoning of mountain territories. *Journal of Geophysics* 43: 227-233.
- [2] Allen C. R., Gilepsil A. R., Han Yuan, Sieh K. E., Buchun Zhang and Zhu Chengnan (1984), "Red River and associated faults, Yuannan Province, China: Quaternary geology, slip rate and seismic hazard". *Geol. Soc. Am. Bull.*, Vol 95, p. 886-900.
- [3] Cao Dinh Trieu, Nguyen Huu Tuyen, Pham Nam Hung, Le Van Dung, Mai Xuan Bach, Giuliano F. Panza, A. Peresan, F. Vaccari, F. Romanelli, 2008. Some features of seismic activity in Vietnam. *The Journal of the ASEAN Committee on Science & Technology*. ISSN 0217-5460, Vol. 25 No. 1 March 2008, p 95-116.
- [4] Cao Dinh Trieu, Pham Huy Long, 2002. Faulting tectonic in Vietnam territory. *Reference book. 208 pages, the Publish of Science and Technology*.
- [5] Cao Dinh Trieu, Nguyen Huu Tuyen, Le Van Dung, Pham Nam Hung, Mai Xuan Bach and Thai Anh Tuan, 2005. Evolution of faulting tectonic in Southeast Asia. *Journal of Geodesy and Geodynamics*, Vol. 25, No. 1, Beijing, China, p 51- 59.
- [6] Cao Đình Trieu, Nguyen Huu Tuyen, Thai Anh Tuan (2006), The correlation between earth's crust feature and earthquakes activity in the Northwest region Vietnam. *Journal of Earth Science*, Vol 28, No 2, Hà nội, p.155-164.
- [7] Cao Đình Trieu (2005), Geophysical field and Lithosphere structure of Vietnam territory. *Reference book, the Publish of Science and Technology*.
- [8] Cisternas A, Godefroy P, Gvishiani A, Gorshkov A, Kossobokov V, Lambert M, Rantsman E, Sallantin J, Saldano H, Soloviev A, Weber C (1985). A dual approach to recognition of earthquake prone areas in the Western Alps. *Annale Geophysicae* 3 (2): 249-270.
- [9] Dang Thanh Hai, 2003. "The characteristics of geological structure - dynamics crust in Northern Vietnam and earthquake conditions". Ph. D desertation. Hanoi National Library.
- [10] Edward A. Keller and Nicholas Pinter (1996), *Active tectonics, Earthquakes, Uplift and Landscape*, Prentice Hall Upper Saddle River, 07458 New Jersey.
- [11] Gabrielov A, Keilis-Borok V, Jackson D (1996). Geometric incompatibility in a fault system. *Proceedings of the USANationalAcademy of Sciences* 93: 3838-3842.
- [12] Gelfand I, Guberman Sh, Izvekova M, Keilis-Borok V, Rantsman E (1972). Criteria of high seismicity, determined by pattern recognition. *Tectonophysics* 13: 415-422.
- [13] Gelfand I, Guberman Sh, Keilis-Borok V, Knopoff L, Press F, Rantsman E, Rotwain I, Sadovsky A (1976). Pattern recognition applied to earthquake epicentres in California. *Physics of the Earth and Planet Interiors* 11: 227-283.
- [14] Gorshkov AI, Kuznetsov IV, Panza GF, Soloviev AA, (2000). Identification of future earthquake sources in the Carpatho-Balkan orogenic belt using morphostructural criteria. *Pure and Appl. Geophysics* 157; 79-95.
- [15] Gorshkov AI, Panza GF, Soloviev AA, Aoudia A (2002). Morphostructural zoning and preliminary recognition of seismogenic nodes around the Adria margin in peninsular Italy and Sicily. *Journal of Seismology and Earthquake Engineering* 4 (1): 1-24.
- [16] Gorshkov AI, Kossobokov V, Soloviev AA (2003). Recognition of earthquake prone areas. In: Keilis-Bork V, Soloviev AA (eds) *Nonlinear Dynamics of the Lithosphere and Earthquake Prediction*. Springer, Heidelberg: 235-320.
- [17] Gorshkov AI, Panza GF, Soloviev AA, Aoudia A (2004). Identification of seismogenic nodes in the Alps and Dinarides. *Bollettino della Societa Geologica Italiana* 123: 3-18.

- [18] Gorshkov AI, Panza GF, Soloviev AA, Aoudia A, Peresan A (2009). Delineation of the geometry of the nodes in the Alps-Dinarides hinge zone and recognition of seismogenic nodes ( $M \geq 6$ ). *Terra Nova*, 21 (4), 257-264. doi: 10.1111/j.1365-3121.2009.00879.x.
- [19] Gorshkov A. I., Soloviev A. A., Jiménez M. J., García-Fernández M., and Panza G. F. (2010). Recognition of earthquake-prone areas ( $M \geq 5.0$ ) in the Iberian Peninsula. *Rendiconti Lincei - Scienze Fisiche e Naturali*, 21 (2), 131-162. doi: 10.1007/s12210-010-0075-3.
- [20] Gvishiani A, Gorshkov A, Kossobokov V, Cisternas A, Philip H, Weber C (1987). Identification of Seismically Dangerous Zones in the Pyrenees. *Annales Geophysica* 5 B (6): 681-690.
- [21] Gvishiani A, Gorshkov A, Rantsman E, Cisternas A, Soloviev A (1988). Identification of earthquake-prone-areas in the regions of moderate seismicity. *Nauka, Moscow*, 175 p. [in Russian].
- [22] Hudnut KW, Seeber L, Pacheo J (1989). Cross-fault triggering in the November 1987 Superstition Hills earthquake sequence, Southern California. *Geophysical Research Letters* 16: 199-202.
- [23] Kent C. Condie, 1988. *Plate tectonics and Crustal evolution*. The third edition.
- [24] King G (1986). Speculations on the geometry of the initiation a termination processes of earthquake rupture and its relation to morphology and geological structure. *Pure and Applied Geophysics* 124: 567-583.
- [25] Korzhuev SS (1974). *Morphotectonics and topography of the Earth' surface*. Editorial Nauka, Moscow: 260 pp [in Russian].
- [26] Le Duc An, 1994. *Geomorphology structure of Vietnam (the main land, the mono graph of geography)*. The Publish of Science and technology, Hanoi.
- [27] Le Pichon X., Francheteau J. et Bonnin J., *Plate Tectonics*, Elsevier, 1973, 300 p.
- [28] Ngo Gia Thang, Le Duy Bach, 2009. The characteristics of Cenozoi intraplate orogenic structures (CIOS) of Vietnam. *Journal of Sciences of the Earth*. No 31 (1)-3-2009. Hanoi.
- [29] Ngo Gia Thang, Le Duy Bach, Nguyen Ngoc Thuy (2007), "The feature of vertical deformation during Pliocen-Quaternary period of the Northwest of Vietnam", *Journal of Earth Science*, Vol 29, No 2, Hà nội, p.161-170.
- [30] Ngo Thi Lu, Belousov T. P., Nguyen Huu Tuyen, 2010. The Alpine geodynamics of Northern Vietnam, Southwest Tibet and Pamir. ASC Conference, Hanoi, Vietnam 08-11, October, 2010.
- [31] Nguyen Ngoc Thuy (Investigator) 2005. Seismic zoning for the Northwest of Vietnam. National Project Research KC-08-10, years 2001-2005.
- [32] Nguyen Huu Tuyen, Chu Van Ngoi, Cao Đình Trieu, Le Van Dung, 2010. The geotectonic settings of the Northwest Vietnam and earthquakes activities. *Proceeding of Scientific Conference of Hanoi Natural University of Sciences*, p. 227-244.
- [33] Nguyen Huu Tuyen, Cao Dinh Trieu, Phung thi Thu Hang, 2012a. The active Geodynamics Blocks model case studied for Tuan Giao Area. *Journal of geology*, Vol 331-332 (5-8/2012), p. 145-155, ISSN 0866-7381.
- [34] Nguyen Huu Tuyen, A. I. Gorshkov, Ngo Thi Lu, 2012b. Recognition of Earthquake-prone area ( $M \geq 5.0$ ) applied for North Vietnam and Adjacency. *Journal of Earth Science*, Vol 34, No 3, Hà nội, p. 251-265.
- [35] Nguyen Van Hung, Hoang Quang Vinh, 2001. "Moving characteristics of the Lai Chau - Dien Bien fault zone during Cenozoic". *Journal of Geology, series B*, N0 17 - 18, p 65.
- [36] Peresan A., Vaccari F., Romanelli F., 2008. Establishing appropriate approaches to increase Tsunami preparedness in Vietnam. Report of Vietnam- Italy Co-operation Programme in Science and Technology for the year 2006-2008.
- [37] Rantsman E. Ya, (1979). Sites of Earthquakes and Morphostructures of Mountain Countries. (Editorial Nauka, Moscow: 171 pp. [in Russian].
- [38] Soloviev, A. User's Guide for Programs CODM and PRAL. Second Workshop on Non-Linear Dynamics and Earthquake Prediction, 22 November - 10 December 1993, Trieste: ICTP, 31 pp.
- [39] Soloviev A. A., Gvishiani A. D., Gorshkov A. I., Dobrovolsky M. N., Novikova O. V. (2014). Recognition of Earthquake-Prone Areas: Methodology and Analysis of the Results. *Izvestiya, Physics of the Solid Earth*, Vol. 50, No. 2, pp. 151-168 DOI: 10.1134/S1069351314020116.
- [40] Talwani P (1988) The intersection model for intraplate earthquakes. *Seismological Research Letters* 59: 305-310.
- [41] Talwani P (1999) Fault geometry and earthquakes in continental interiors. *Tectonophysics* 305: 371-379.
- [42] Turcotte D. L, Schubert G., 2002. *Geodynamics (text book)*. Cambridge University Press (Second edition)
- [43] Robert S. Yeats (1997), *The Geology of Earthquakes*. Oxford University Press.
- [44] Tapponnier P, Leloup H. P, Lacassin R (1995), "The Tertiary Tectonic South China and Indochina", The Conference on Cenozoic Evolution of the Indochina Peninsula, HaNoi - Dason, Vietnam.